

# Numerical simulation for DC Schottky gate leakage current in AlGaN/GaN HEMTs

R. Rodríguez, B. González, J. García, A. Núñez

IUMA, ULPGC

Campus Universitario de Tafira S/N, E-35017  
Las Palmas de G.C., Spain  
e-mail: rrodriguez@iuma.ulpgc.es

G. Toulon

Exagan, 51 rue de l'Innovation, 31670

Labège, France; gtoulon@laas.fr

F. Morancho

LAAS-CNRS, Université de Toulouse, CNRS, UPS,  
31400 Toulouse, France; morancho@laas.fr

**Abstract**— Different causes of the gate leakage origin in AlGaN/GaN HEMTs on Si have been studied through numerical simulations. Based on DC measured results and employing Sentaurus Device, different trap effects under the Schottky gate must be included to reproduce the measured transfer characteristics in subthreshold regime. Additionally, numerical simulation aspects for GaN-based HEMTs are also detailed.

**Keywords**—TCAD, AlGaN/GaN HEMT on Si, trapping effects, Schottky gate

## I. INTRODUCTION

III-V semiconductors are the basis of high-frequency, high temperature and high power applications in the power inverters and power amplifiers to come [1-3]. Thus, in order to achieve the expected results by the telecommunication and electronic industry, an in-depth knowledge of TCAD use is fundamental in radio frequency and high power circuitry.

Obtained results on GaN manufacturing are being encouraging. However, defects and traps still may appear in the epitaxial processing and crystal growth, which leads to undesired collateral effects such as current collapse and leakage current, among others [4]. Particularly, diminishing of the off-state leakage current in HEMT devices conditions their integration into circuits, in which low noise and low power consumption are important figures of merit. Accurate determination of trapping effects is an appropriate way to ensure the electrical functionality of these devices, in order to engineer reliable circuit designs [5-7].

Trapping effects can be caused by the etching process for Schottky gates, together with electrical stress during normal device operation that entails to provoke traps in barriers.

In this work, the HEMT structure is presented in Section 2. A trapping effect review is exposed in Section 3. TCAD simulations are explained in Section IV, together with the evaluation of trap concentration and distribution. Finally, conclusions are summarized in Section 4.

## II. ALGAN/GAN STRUCTURE

In this work, the study is focused on a normally-on HEMT on silicon [8], based on the AlGaN/GaN system, 1000 μm wide, with the technological processing carried out at LAAS. Source-to-gate and gate-to-source distances are, respectively, 2 and 5 μm, with a Schottky gate 2 μm long.

The layer stack of the device is shown in Fig. 1, where the donor doping concentration,  $N_D$ , and the layer thickness

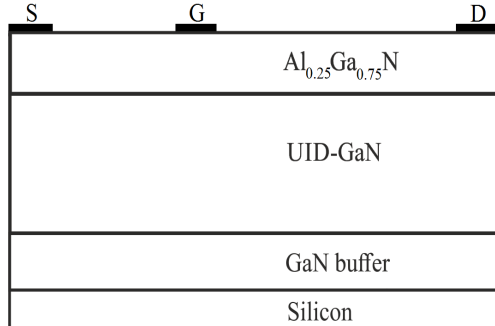


Fig. 1. Simulated normally-off HEMT based on GaN.

of the different layers are indicated in Table I. Notice that below the AlGaN barrier and GaN channel, a practically undoped GaN buffer (with similar electrothermal performance) substitutes the transition layers for simulation purposes.

## III. TRAPPING EFFECTS REVIEW

Three notable mechanisms exist for gate leakage current, according to the literature. Fowler-Nordheim (FN) [9], the simplest tunneling model, is given by:

$$j_{FN} = AF^2 \exp\left(-\frac{B}{F^2}\right) \quad (1)$$

where  $j_{FN}$  is the tunnel current density,  $F$  the electric field at the interface under the gate, and  $A$  and  $B$  are physical constants depending on the material and its molar fraction, Al<sub>0.25</sub>Ga<sub>0.75</sub>N in our case, as in [10], with  $A = 1.53 \cdot 10^{-6}$  A/V<sup>2</sup> and  $B = 2.17 \cdot 10^8$  V/cm.

Poole-Frenkel emission (PF) [11] is an emission transport through a continuum of trap states, which is sensitive to the temperature and the electric field and, therefore, difficult to identify at low bias in the subthreshold region. It is modeled as:

$$\sigma_n^{enh} = \sigma_n^0 (1 + \Gamma_{pf}) \quad (2)$$

$$\Gamma_{pf} = \frac{1}{\alpha^2} [1 + (\alpha - 1)\exp(\alpha)] - \frac{1}{2} \quad (3)$$

$$\alpha = \frac{1}{kT} \sqrt{\frac{q^3 F}{\pi \epsilon_{pf}}} \quad (4)$$

TABLE I. THICKNESS AND DOPING OF THE DEVICE.

Layer	Thickness (nm)	n-doping (cm <sup>-3</sup> )
AlGaN	30	10 <sup>15</sup>
UID-GaN	1100	10 <sup>16</sup>
GaN buffer	500	10 <sup>12</sup>

where the emission probability for charged trap centers is given by  $\Gamma_{\text{pf}}$ ,  $\sigma_n^{\text{enh}}$  and  $\sigma_n^0$  are the donor and electron-neutral concentration traps, respectively, and  $\epsilon_{\text{pf}}$  is a characteristic permittivity for the PF model. All these parameters are set by default by the simulator [10].

Finally, in Trap Assisted Tunneling (TAT) emission [12] most of tunneling takes place through a two-step tunneling via a mid-band state-layer of scattered traps within the AlGaN barrier layer [13]. The lifetime,  $\tau$ , and capture cross section,  $\sigma$ , become function of the trap-assisted tunneling factor,  $\Gamma_{\text{tat}}$ , as

$$\tau = \tau_0 / (1 + \Gamma_{\text{tat}}) \quad (5)$$

$$\sigma = \sigma_0 / (1 + \Gamma_{\text{tat}}) \quad (6)$$

where  $\Gamma_{\text{tat}}$  is given by:

$$\Gamma_{\text{tat}} = \int_0^{\tilde{E}_n} \exp \left[ u - \frac{2\sqrt{u^3}}{3\tilde{E}} \right] du \quad (7)$$

with  $\tilde{E}$  and  $\tilde{E}_n$  defined as:

$$\tilde{E} = \frac{E}{E_0}, \text{ where } E_0 = \sqrt{\frac{8m_0 m_t k^3 T^3}{q\hbar}} \quad (8)$$

$$\tilde{E}_n = \frac{E_n}{kT} \quad (9)$$

where  $m_t$  is the carrier tunneling mass and  $E_n$  is a characteristic energy depending on the Fermi level position as in [10].

Finally, it is known that the etching process in GaN-based devices, during a Schottky gate contact formation, can lead to defective adhesion properties at the metal/semiconductor interface, originating traps under the gate. Additional trapping under the gate can be caused by electrical stress [14, 15], which is present in the (across the barrier) gate edge region of the HEMT under study. Thus, a trap concentration  $t$  depth under the gate of the transistor investigated is considered.

#### IV. TCAD RESULTS

TCAD simulations have been developed with Sentaurus Device (from Synopsys) [16]. The impact of SHEs on the transistor DC response has been in-depth analyzed by auto-consistently solving the heat flow equation together with the Poisson and drift-diffusion equations, as in [17].

A thermodynamic model is used by Sentaurus Device to compute a non-uniformly distributed lattice temperature, whose equations are given by:

$$\begin{aligned} \frac{\partial}{\partial t} (c_L T) - \nabla \cdot (\kappa \nabla T) = \\ -\frac{1}{q} \left( E_C + \frac{3}{2} kT \right) (\nabla \cdot \vec{J}_n - q R_{\text{net},n}) \end{aligned} \quad (10)$$

$$-\frac{1}{q} \left( E_V + \frac{3}{2} kT \right) (-\nabla \cdot \vec{J}_p - q R_{\text{net},p}) + \omega \hbar G^{\text{opt}}$$

where  $\kappa$  is the thermal conductivity,  $c_L$  is the lattice heat capacity,  $E_C$  and  $E_V$  are the conduction and valence band energies, respectively;  $G^{\text{opt}}$  is the photon optical generation rate at the frequency  $\omega$ , and  $R_{\text{net},n}$  and  $R_{\text{net},p}$  are the electron and hole net recombination rates, respectively.

Total polarization in III-V materials is determined as [18]

$$P = P_{\text{SP}} + P_{\text{PZ}} \quad (11)$$

where  $P_{\text{SP}} = p_{\text{sp}} \cdot z$  is the spontaneous polarization, with  $p_{\text{sp}}$  being the spontaneous polarization charge (-0.029 C/m<sup>2</sup> for GaN in wurtzite crystal; in the case of the AlGaN value it is assumed as an interpolation from AlN and GaN).  $P_{\text{PZ}}$  is the strain polarization, which can be calculated from the piezoelectric coefficients  $e_{33}$  and  $e_{31}$ , and the elastic constants  $c_{13}$  and  $c_{33}$ .

With Sentaurus solving numerically the heat equation within a 2D drift-diffusion transient scheme (due to the traps dynamic response) at room temperature, the physical models must be set considering the Schottky gate and the AlGaN/GaN heterostructure. Thus, the Masetti mobility model [19] is used for electrons at low electric fields, to account for the  $n$ -doping and lattice temperature dependencies as follows:

$$\begin{aligned} \mu_{\text{dop}} = \mu_{\text{min1}} \exp \left( -\frac{P_c}{N_{A,0} + N_{D,0}} \right) \\ + \frac{\mu_{\text{const}} - \mu_{\text{min2}}}{1 + ((N_{A,0} + N_{D,0})/C_r)^{\alpha}} - \frac{\mu_1}{1 + (C_s/(N_{A,0} + N_{D,0}))^{\beta}} \end{aligned} \quad (12)$$

where  $N_{A,0}$  and  $N_{D,0}$  are the acceptor and donor doping concentrations, respectively,  $\mu_{\text{const}}$  is the low-doping reference mobility, which is determined by

$$\mu_{\text{const}} = \mu_L \left( \frac{T}{300\text{K}} \right)^{-\zeta} \quad (13)$$

with  $\mu_L$  being the mobility due to bulk phonon scattering at

TABLE II. MODEL PARAMETERS

Parameter	Electron	Hole	Units
$\mu_L$	1500	30	cm <sup>2</sup> /Vs
$\mu_{\text{min1}}$	85	33	cm <sup>2</sup> /Vs
$\mu_{\text{min2}}$	75	0	cm <sup>2</sup> /Vs
$\mu_1$	50	20	cm <sup>2</sup> /Vs
$P_c$	$6.5 \times 10^{15}$	$5 \times 10^{15}$	cm <sup>-3</sup>
$C_r$	$9.5 \times 10^{16}$	$8 \times 10^{16}$	cm <sup>-3</sup>
$C_s$	$7.2 \times 10^{19}$	$8 \times 10^{20}$	cm <sup>-3</sup>
$\alpha$	0.55	0.55	1
$\beta$	0.75	0.7	1

room temperature. All parameters of this model have been set for this HEMT, and their values are shown in Table II.

In the case of the AlGaN/GaN heterojunction, for saturation regime, the following nitride specific field dependent mobility model is used [20], with appropriate negative differential mobility due to intervalley transfers at high electric fields [21]:

$$\mu = \frac{\mu_{\text{dop}} + v_{\text{sat}} \frac{F^{\beta-1}}{E_1^\beta}}{1 + \gamma \left( \frac{F}{E_0} \right)^\alpha + \left( \frac{F}{E_1} \right)^\beta} \quad (14)$$

where  $E_0$ ,  $E_1$  and  $v_{\text{sat}}$ , the saturation velocity, are the parameters giving rise to a variation of the peak velocity and peak electric field as well as the steepness of  $v(F)$  in the saturation region.

In order to be rigorous using this model, the parameters for GaN and  $\text{Al}_{0.25}\text{Ga}_{0.75}\text{N}$  have been set according to the doping and molar fraction of this device, as shown in Table III.

The thermionic current model for electrons and holes, (15) and (16), is active at all semiconductor interfaces. Thermionic-Emission (TE) [22] assumes that, at heterointerfaces, the conduction band energy discontinuity is positive,  $\Delta E_C > 0$ . If  $J_{n,2}$  is the electron current density entering material 2 and  $J_{n,1}$  the electron current density leaving material 1, the interface condition is:

$$J_{n,2} = J_{n,1} \quad (15)$$

$$J_{n,2} = a_n q \left( v_{n,2} n_2 - \frac{m_{n,2}}{m_{n,1}} v_{n,1} n_1 \exp \left( -\frac{\Delta E_C}{kT} \right) \right) \quad (16)$$

with  $a_n$  being a fitting coefficient,  $m_{n,i}$  are the effective masses of the electron,  $n_i$  the electron concentration, and  $v_{n,i}$  are the electron emission velocities, which are defined as:

$$v_{n,i} = \sqrt{\frac{kT_{n,i}}{2\pi m_{n,i}}} \quad (17)$$

A gate Schottky diode with Poole–Frenkel (PF) emission is considered for all operating regimes [23]. Therefore, the gate current is given by:

$$J_{n,2} = a_n q \left( v_{n,2} N_{c,2} \zeta_{n,2} - \frac{m_{n,2}}{m_{n,1}} v_{n,1} N_{c,1} \zeta_{n,1} \right) \quad (18)$$

where  $N_{c,1}$  and  $N_{c,2}$  are the effective density of states in the

TABLE III. HETEROJUNCTION PARAMETERS

Parameter	GaN	$\text{Al}_{0.25}\text{Ga}_{0.75}\text{N}$	Units
$E_0$	$22.09 \times 10^4$	$26.56 \times 10^4$	V/cm <sup>-1</sup>
$E_1$	220893.6	265579.4	V/cm <sup>-1</sup>
$\alpha$	0.78	0.79	1
$\beta$	7.20	8.12	1
$\gamma$	6.19	7.32	1

conduction band for both materials, and  $\zeta_{n,2}$  and  $\zeta_{n,1}$  are correction parameters. High carrier densities together with a moderate density-of-states require all simulations to be performed with Fermi statistics.

When using ohmic contacts at source/drain terminals, nonphysical bending would take place, due to charge neutrality condition, where the contacts cross the heterointerface, deriving simulations without convergence with Sentaurus Device. Thus, to avoid convergence glitches, source/drain contacts are implemented as Schottky contacts and carriers are allowed to tunnel into the device with a reduced effective electron mass [10, 23], as Figure 2 shows.

It is well known that in the surface of the AlGaN layer, the crystal discontinuity may provoke surface states. This effect is managed as a donor sheet density of  $2.3 \times 10^{13} \text{ cm}^{-2}$ , with an activation energy of 0.4 eV from the middle of the band gap. In the GaN buffer, in order to form an intrinsic material, with an insulator nature, a compensation is performed by incorporating impurities. But this method typically introduces acceptor traps. To consider this, an acceptor trap concentration of  $10^{17} \text{ cm}^{-3}$  has been incorporated into the GaN buffer, with an activation energy from the conduction band minimum of 3 eV [5].

In order to fit the threshold voltage as in [24], a donor traps layer has been introduced under the gate metal. This layer has a thickness of 2 nm, and the traps located here have a capture cross-section of  $10^{-15} \text{ cm}^{-2}$  and an activation energy of 3.2 eV, from the valence band maximum.

Thus, as Figure 3 shows, measured (with symbols) and simulated (with solid line) transfer characteristics, which are represented in logarithmic scale, coincide in strong inversion regime, above threshold voltage. However, the existence in subthreshold regime of a constant leakage current,  $I_{\text{off}}$ , of  $22.5 \mu\text{A}$  is not being numerically reproduced, even when non-local tunneling with FN emission through the gate is activated in simulations (with dashed lines) [22, 24]. Nevertheless,  $I_{\text{off}}$  can be better predicted if, additionally, the donor layer thickness for traps under the gate,  $t$ , is incremented. This effect is observed in Figure 3, where transfer characteristic is represented for  $t = 4 \text{ nm}$  (with dotted line). Thus, the difference between measured and simulated subthreshold current is reduced in more than five orders of magnitude.

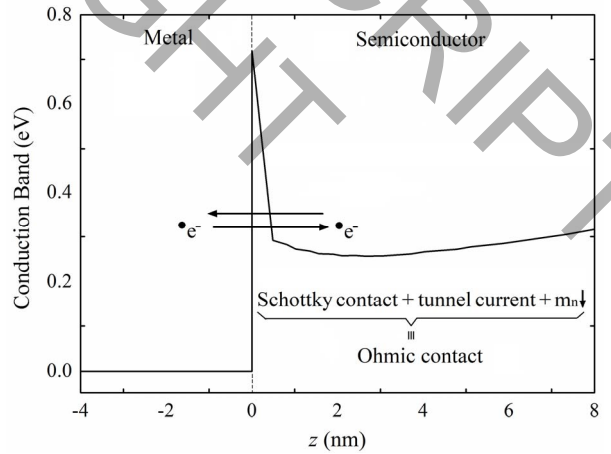


Fig. 2. Conduction band diagram below the source/drain contacts, implemented as a Schottky contact with tunnel current and reduced effective mass of the carriers.

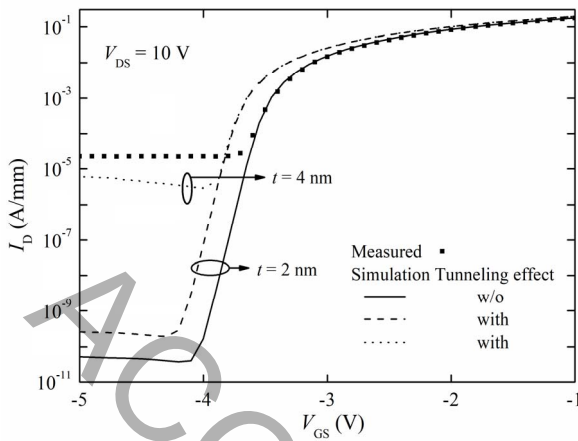


Fig. 3. Measured (symbols) and simulated (solid/dashed line without/with tunneling effect) transfer characteristics for the AlGaN/GaN HEMT;  $V_{DS} = 10$  V.

In an off-state regime, gate and drain measured currents coincide with all leakage current flowing through the gate being collected by the drain terminal, across the GaN channel [25].

## V. CONCLUSION

A detailed explanation about numerical simulation of DC-characteristics of AlGaN/GaN-based HEMTs, with Sentaurus Device, has been exposed.

All terminals were modeled as Schottky contacts showing tunnel current and, in the case of the gate, additional Poole-Frenkel and non-local tunneling with Fowler-Nordheim emissions are necessary.

Trapping effects are crucial to be set. Thus, trap concentration, distribution and activation energy were determined. Below the gate, a local donor trap density was tuned in order to reproduce the leakage current, maintaining a correct prediction for the drain current in strong inversion regime.

## ACKNOWLEDGMENT

This work was supported in part by MINECO (TEC2015-71072-C03-01) and by ACIISI (ProID2017010067).

## REFERENCES

- [1] S. Chander, et al., "M. 30 nm Normally off enhancement mode AlGaN/GaN HEMT on SiC substrate for future high speed nanoscale power applications", In Proceedings of the 2017 International Conference on Innovations in Electrical, Electronics, Instrumentation and Media Technology (ICEEIMT), Coimbatore, India, 3–4 February 2017; pp. 293–296.
- [2] J.W. Chung, et al., "Advanced gate technologies for state-of-the-art fT in AlGaN/GaN HEMTs". In Proceedings of the 2010 International Electron Devices Meeting, San Francisco, CA, USA, 6–8 December 2010; pp. 30.2.1–30.2.4.
- [3] G. Meneghesso, et al., "Reliability of GaN high-electron-mobility transistors: State of the art and perspectives". IEEE Trans. Device Mater. Reliab. 2008, 8, 332–343.
- [4] K. Mukherjee, et al., "TCAD simulation capabilities towards gate leakage current analysis of advanced AlGaN/GaN HEMT devices", Microelectron. Reliab. 2017, 76–77, 350–356.
- [5] D. Bisi, et al., "Deep-Level Characterization in GaN HEMTs—Part I: Advantages and Limitations of Drain Current Transient Measurements", IEEE Trans. Electron Devices 2013, 60, 3166–3175.
- [6] A. Chini, et al., "Deep Levels Characterization in GaN HEMTs—Part II: Experimental and Numerical Evaluation of Self-Heating Effects on the Extraction of Traps Activation Energy", IEEE Trans. Electron Devices 2013, 60, 3176–3182.
- [7] D. Cornigli, et al., "Numerical investigation of the lateral and vertical leakage currents and breakdown regimes in GaN-on-Silicon vertical structures", In Proceedings of the 2015 IEEE International Electron Devices Meeting (IEDM), Washington, DC, USA, 7–9 December 2015; pp. 5.3.1–5.3.4.
- [8] S. Hamady, et al., "Scalable normally-off AlGaN/GaN HEMT using fluorine implantation below the channel", In Proceedings of the Symposium de Génie Electrique (SGE 2014), ENS Cachan, France, 8–10 July 2014.
- [9] M. Lenzlinger, et al., "Fowler-Nordheim Tunneling into Thermally Grown SiO<sub>2</sub>", J. Appl. Phys. 1969, 40, 278.2.
- [10] Synopsys Inc. Sentaurus device user guide, Version N-2017.09. 2017.
- [11] L. Colalongo, et al., "Numerical Analysis of Poly-TFTs Under Off Conditions", Solid-State Electron. 1997, 41, 627–633.6.
- [12] A. Schenk, "A Model for the Field and Temperature Dependence of Shockley–Read–Hall Lifetimes in Silicon", Solid-State Electron. 1992, 35, 1585–1596.
- [13] J. Kotani, et al., "Mechanism of surface conduction in the vicinity of Schottky gates on heterostructures", Appl. Phys. Lett. 2007, 91, 093501.
- [14] J. Joh, et al., "Impact of electrical degradation on trapping characteristics of GaN high electromobility transistors", In Proceedings of the 2008 IEEE International Electron Devices Meeting, San Francisco, CA, USA, 15–17 December 2008; pp. 1–4.
- [15] J. Joh, et al., "Mechanisms for Electrical Degradation of GaN High-electron Mobility Transistors", In Proceedings of the 2006 IEEE International Electron Devices Meeting, San Francisco, CA, USA, 11–13 December 2006; pp. 1–4.
- [16] R. Rodríguez, et al., "Electrothermal DC characterization of GaN on Si MOS-HEMTs", Solid-State Electron. 2017, 137, 44–51.
- [17] O. Ambacher, et al., "Two dimensional electron gases induced by spontaneous and piezoelectric polarization in undoped and doped AlGaN/GaN heterostructures", J. Appl. Phys. 2000, 87, 334–344.
- [18] G. Masetti, et al., "Modeling of Carrier Mobility Against Carrier Concentration in Arsenic-, Phosphorus-, and Boron-Doped Silicon," IEEE Transactions on Electron Devices, vol. ED-30, no. 7, pp. 764–769, 1983.
- [19] M. Farahmand, et al., "Monte Carlo simulation of electron transport in the III-nitride wurtzite phase materials system: binaries and ternaries", IEEE Trans Electron Devices 2001;48:535–42.
- [20] J.M. Barker, et al., "Bulk GaN and AlGaN/GaN heterostructure drift velocity measurements and comparison to theoretical models", J Appl Phys 2005;97.
- [21] S. Turuvekere, et al., "Gate Leakage Mechanisms in AlGaN/GaN and AlInN/GaN HEMTs: Comparison and Modeling", IEEE Trans. Electron Devices 2013, 60, 3157–3165.
- [22] D. Schroeder, "Modelling of Interface Carrier Transport for Device Simulation", 1st ed.; Springer: Wien, Austria, 1994; ISBN 978-3-7091-7368-8.4.
- [23] Sze, S.M. MOSFET. In Physics of Semiconductor Devices; Wiley: New York, NY, YSA, 1981.
- [24] J. Jungwoo, "Physics of electrical degradation in GaN high electron mobility transistors", Ph.D. Thesis, Massachusetts Institute of Technology, Cambridge, MA, USA, 2009.
- [25] R. Rodríguez, et al., "DC Gate Leakage Current Model Accounting for Trapping Effects in AlGaN/GaN HEMTs", Electronics. 2018, 7, 210.